Identification of the modal and structural properties of a high-rise scale model

A.J. Bronkhorst [1], **E. Marchelli** [2], **D. Moretti** [1], **K. Maes** [3], **G. Lombaert** [3]
[1] TNO, Department of Reliable Structures,
Molengraaffsingel 8, 2629 JD, Delft, The Netherlands,
e-mail: **okke.bronkhorst@tno.nl**

[2] Università degli Studi di Genova, Civil, Chemical and Environmental Engineering Department,
Villa Cambiaso, Via Montallegro 1, 16145, Genoa, Italy

[3] KU Leuven, Department of Civil Engineering,
Kasteelpark Arenberg 40, B-2448, Leuven, Belgium

Abstract
The fundamental natural frequency of high-rise buildings is crucial for predicting wind-induced vibrations that affect living and working conditions. It is often underestimated during design. To explore the discrepancy between predicted and measured natural frequencies, model updating was applied to several Dutch high-rise buildings. This revealed challenges in estimating building and foundation stiffness reliably using model updating. A laboratory experiment with a scale model was conducted to replicate in-situ interactions and generate modal property data for different structural configurations. Model updating was applied to configurations with a fixed, stiff spring, and soft spring base. Results show that increased base flexibility makes shear stiffness estimates highly sensitive, while axial stiffness remains stable. These findings suggest that model updating can estimate in-situ rotational foundation stiffness effectively but is less reliable for horizontal stiffness. Future research will extend these investigations to both the test structure and in-situ buildings.

1 Introduction

For high-rise buildings, accurately predicting the first bending natural frequency is essential when estimating the wind-induced dynamic response. Studies on the wind-induced dynamic behaviour of high-rise buildings [1][2][3] have shown that the fundamental natural frequency computed in design can differ as much as a factor of 1.5 to 2 from the natural frequency determined from in-situ measurements. Underestimating the fundamental natural frequency in the design phase can result in overly conservative designs, i.e. in the most extreme case an underestimation of the natural frequency by a factor of 2 translates to an underestimation of the overall bending stiffness by a factor 4. It is unclear whether these underestimations are the result of an inaccurate prediction of the building mass, building stiffness or foundation stiffness properties. It is desirable from a design and economic point of view to determine the cause of these differences and reduce this uncertainty in models of high-rise buildings.

According to Friswell and Mottershead [4], model updating is a procedure to modify a model to better reproduce the measured response of the actual structure. This procedure can for example be used to investigate the cause of discrepancies between the modal characteristics predicted using a model and those derived from measurements. The updated structural properties minimise the difference between modelled and measured modal characteristics. The reliability of these estimated structural properties is highly dependent on the available set of measured modal characteristics (natural frequencies and mode shapes), as well as the representativeness of the model that is being updated. Therefore, it is useful to test model updating in a controlled environment and on structures in which the actual stiffness and mass properties can be measured accurately.

The aims of this study are to (i) generate a dataset that can be used to benchmark model updating techniques, (ii) explore the sensitivity of the different parameters selected for the model updating, and (iii) investigate the link between a considered set of modal data and the quality of identified parameter values.

Section 2 provides a more in-depth discussion on the mismatch between modal properties estimated in design and those obtained from vibration measurements, and discusses the application of model updating of high-rise buildings based on in-situ measured modal properties. Section 3 presents a conceptual high-rise lab-scale model, i.e. the test structure, which was developed to study the application of model updating for structural identification on a tall slender structure with flexible base. The measurements performed for various configurations (i.e. support stiffness and column arrangements) of this test structure are described, as well as various versions of the finite element model of the structure. Section 4 presents and discusses results of the comparison between the modelled and measured modal characteristics. Section 5 gives conclusions and recommendations for future work.

2 Background

2.1 Prediction natural frequency high-rise buildings

The main dynamic characteristics of a building that influence wind-induced vibrations are the natural frequency, mode shape, and damping ratio of the fundamental bending mode. Various studies that compared the in-situ measured natural frequencies of high-rise buildings with those computed in the design phase observed significant differences. For example, Ellis [5] found that differences of 50% between computed and measured in-situ natural frequencies are common. Ellis furthermore noted that empirical relations often provide more accurate estimates for the fundamental natural frequency than predictions based on computer models. In current design practice, the natural frequencies are generally determined with a FEM model. Studies, for example by Kijewski-Correa et al. [6], Kim et al. [3], and Zhou et al. [7], observed that it is also quite difficult to make accurate FEM based predictions of the natural frequency in the design phase.

In the research project HiViBe (High-rise ViBrations in delta cities explored) measurements and calculations are performed on several high-rise buildings in the Netherlands. The aim is to improve modelling approaches in engineering practice. Table 1 gives information about the superstructure and the foundation of some of the high-rise buildings investigated in this research project. Figure 1 shows a side view of the buildings, indicating the instrumented floors. The cross sections show the main load-bearing elements in each of the buildings and indicate the coordinate system. The residential tower New Orleans has a permanent monitoring system on the 34^{th} floor, which was temporarily supplemented with additional acceleration sensors on the 15^{th} and 44^{th} floor. The New Erasmus Medical Center (NEMC) was equipped with acceleration sensors on the top floor. The Zalmhaven I is also instrumented with a permanent monitoring system on the 1^{st} and 58^{th} floor since January 2022; additional sensors were placed on the 20^{th}, 25^{th} and 30^{th} floor for a few months. The JuBi tower was instrumented with accelerometers on the 9^{th}, 22^{nd} and 37^{th} floor and strain gauges on the 9^{th} floor. The accelerometers on the Montevideo tower were installed on the 27^{th} and 42^{nd} floor. The natural frequencies and mode shapes of the buildings were obtained from the acceleration measurements with the Frequency Domain Decomposition (FDD) technique. Table 2 gives the measured and computed natural frequencies, as well as the dominant direction of the corresponding mode shapes. The results for the natural frequencies show that the numerical models of all buildings underestimate the measured values.

Table 1: General information on the studied high-rise buildings in the HiViBe project.

High-rise (City)	New Orleans (Rotterdam)	JuBi tower (The Hague)	NEMC (Rotterdam)	Zalmhaven I (Rotterdam)
Height	155 m	146 m	120 m	215 m
Width	28 m	50 m	45 m	35 m
Depth	28 m	38 m	21 m	35 m
Pile number	316	521	352	163
Pile section	0.45 m	0.45/0.4 m	0.45 m	0.76-0.95 m
Pile length	21 m	8 m	18.5 m	64 m

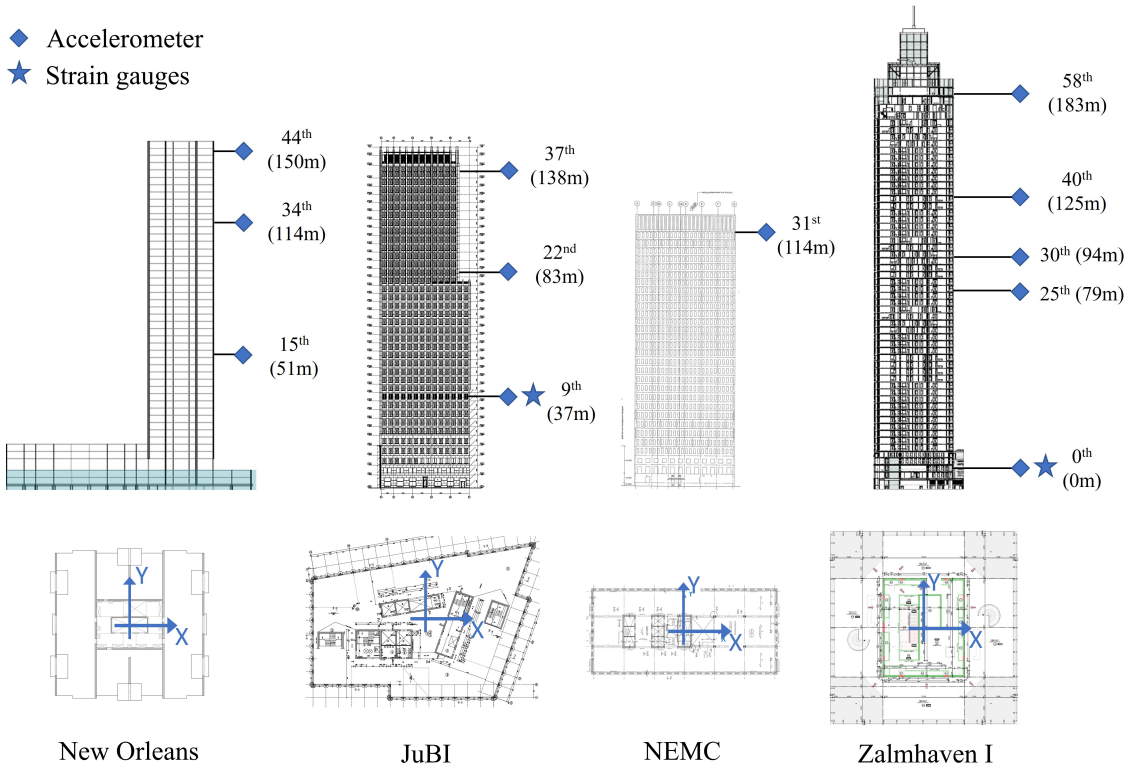

Figure 1: Buildings investigated in the HiViBe project: (a) New Orleans, (b) JuBi tower, (c) New Erasmus Medical Center (NEMC), and (d) Zalmhaven I.

Table 2: Computed and measured natural frequencies of the high-rise buildings.

Mode	New Orleans		JuBi tower		NEMC		Zalmhaven I	
	FEM	Meas.	FEM	Meas.	FEM	Meas.	FEM	Meas.
1	0.20-X	0.28-Y	0.34-Y	0.39-Y	0.27-Y	0.54-Y	0.24-X	0.34-X
2	0.23-Y	0.29-X	0.47-X	0.56-X	0.44-X	0.68-X	0.25-Y	0.34-Y
3	0.50-ϑ	0.64-ϑ	0.76-ϑ	0.92-ϑ	0.74-ϑ	1.30-ϑ	0.52-ϑ	0.63-ϑ
4	1.02-X	1.33-X	1.27-Y	1.40-Y	1.19-Y	1.97-—	1.23-Y	1.26-Y
5	1.25-Y	1.53-Y	1.65-X	2.05-X	1.64-X	2.17-—	1.25-X	1.44-X
6	1.55-ϑ	2.01-ϑ	2.14-ϑ	2.45-ϑ	2.26-ϑ	2.83-ϑ	1.51-ϑ	1.86-ϑ

2.2 Application of model updating for structural identification high-rise buildings

Model updating can be used to estimate in-situ structural properties from vibration measurements. This is achieved by minimising the difference between the modal properties of a structural model and those measured on the structure. Various studies have applied model updating to estimate structural properties of high-rise structures. Wu and Li [8] applied model updating on a FEM model of an 310 m tall TV tower, with the aim of obtaining a more accurate model of the tower for the assessment of the wind induced response after it was observed that measured wind induced accelerations exceeded the comfort limit, due to an inaccurate design estimate of the natural frequencies. Ventura et al. [9] conducted model updating on a 15-story reinforced concrete shear core building, the Heritage Court Tower in Vancouver. They employed modal characteristics extracted after conducting a series of ambient vibration tests by the University of British Columbia. Kaynardag and Soyöz [10] used model updating on the FEM model of an existing tall building to more accurately assess the seismic performance. Moretti et al. [11] performed parameter identification to estimate the in-situ structural properties of the New Orleans tower from the measured ambient vibrations. In this study, the mass and bending stiffness of the building as well as the foundation stiffness were updated. The results suggested that the underestimation of the first natural frequencies of this building were mainly caused by an underestimation of the building and foundation stiffness. However, the rotational foundation stiffness determined deviated almost an order of magnitude from the value applied in design. Moretti et al. [11] attributed this large deviation to the simplified building model, which has a uniform stiffness over the height and does not consider the frequency dependence of the foundation stiffness. Recent results of this work suggest however that the large deviation is more likely a uniqueness issue. Table 3 presents new results for the New Orleans tower, as well as the other towers. These results were obtained with the same model as described in [11], but only the building stiffness and foundation stiffness were updated, and the building mass was kept fixed at the design value. For the New Orleans building, the updated stiffness values do not deviate by an order of magnitude from the design values. Nevertheless, for some of the other buildings, very large differences are observed, as can be seen in Table 3 for the NEMC. Because of these differences and the fact that the actual in-situ values are not known, we have doubts about the reliability of the results presented in Table 3. More research is needed to determine how we can distinguish between errors in building and foundation stiffness. To this end, a laboratory experiment has been set up with a scale model of a high-rise building, in which the influence of a flexible base is present in a similar way as in real buildings.

Table 3: Global structural properties of three high-rise buildings obtained from FEM calculations and with model updating.

Parameter	New Orleans		NEMC		Zalmhaven I	
	FEM	MU	FEM	MU	FEM	MU
ρ [kg/m^3]	477	477	455	455	330	330
EI_{xx} [GN/m^2]	7.1E+4	15.5E+4	8.9E+4	20.5E+4	15.7E+4	27.4E+4
EI_{yy} [GN/m^2]	5.4E+4	13.1E+4	3.1E+4	25.6E+4	15.7E+4	25.1E+4
$K_{r,xx}$ [GNm/rad]	2.0E+3	2.5E+3	2.1E+3	6.2E+3	7.1E+3	15.4E+3
$K_{r,yy}$ [GNm/rad]	1.9E+3	3.4E+3	7.0E+3	56.6E+3	7.1E+3	18.7E+3
$K_{t,x}$ [GN/m]	3.10	1.55	5.88E	1.91	∞	3.09
$K_{t,y}$ [GN/m]	3.10	2.19	5.56	3.13	∞	2.19

3 Laboratory experiment

3.1 Test structure

The test structure is a simplified scale model of a tower. It is a five-story steel frame, built with modular elements of different dimensions, as illustrated in Figure 2(a). The structure is built from vertical column strips with rectangular cross-sections and horizontal floor plates bolted together using angular L-shaped corner connectors, as displayed in Figure 2(b). At the bottom of the model, two 6.2 mm thick steel strips are connected to the columns. The reference system applied in the measurements is illustrated in Figure 2(b); the same reference system is employed for the FE model of the test structure. Model setups investigated in the tests differ according to the boundary conditions at the base and the thickness t of the vertical column strips on one side of the model, which can be 1.5 or 2 mm thick. Table 4 specifies the investigated model setups. The different configurations of columns are labelled from C1 to C7. Table 4 specifies for each configuration the relative amount of 1.5 mm columns. Figure 2(a) displays configuration C1, where one side of the model is fully made up of the red columns, which have a thickness of 1.5 mm, and the other side has yellow columns with a thickness of 2 mm. In the other configurations, the red columns are progressively replaced by the 2.0 mm thick columns. The width b of the columns is 25.1 mm. The arrangement of the cross-section of the columns implies that the structure is more flexible in the x-direction than in the y-direction. Different base boundary conditions were considered in the tests. Besides a fixed base condition, two flexible base conditions were investigated. The fixed base conditions (setup 01 to 07) were obtained by connecting the horizontal beams to a rail at the same points where the springs were bolted for the other setups. In setup 08 to 15, four neoprene springs of the same stiffness were bolted under the horizontal steel strips. Two pairs of four springs were used, differing in axial and shear stiffness, allowing two different flexible base conditions. Stiff rubber bobbins (product code 5020VV25) with a shear and axial stiffness of 133000 N/m and 580000 N/m were used to represent a stiff base condition. Soft rubber bobbins (product code 4035VV25) with a shear and axial stiffness equivalent to 24000 N/m and 127000 N/m were used for a soft base condition.

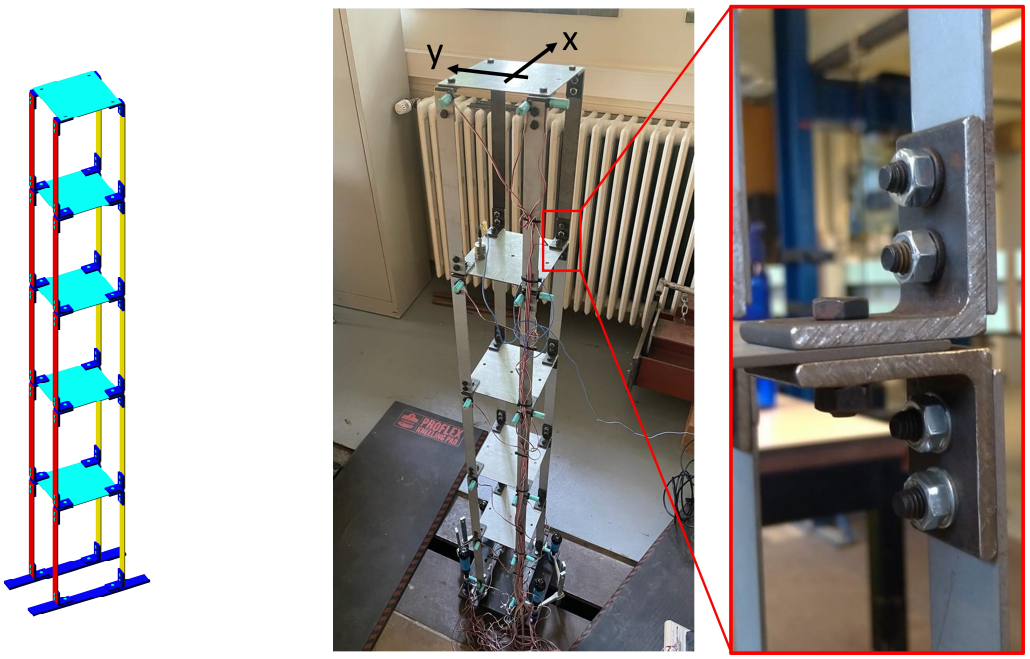

(a) (b)

Figure 2: (a) AutoCAD drawing of the test structure, (b) picture of the instrumented test structure and detail of corner connectors.

Table 4: Description of test structure setups investigated in the experiments.

Setup	% 1.5mm columns	Configuration	Base conditions
01	100	C1	Fixed
02	90	C2	Fixed
03	80	C3	Fixed
04	60	C4	Fixed
05	40	C5	Fixed
06	30	C6	Fixed
07	20	C7	Fixed
08	20	C7	Soft
09	30	C6	Soft
10	40	C5	Soft
11	20	C7	Soft
12	20	C7	Stiff
13	30	C6	Stiff
14	40	C5	Stiff
15	20	C7	Stiff

3.2 System Identification

The response of the structure is measured by twenty-five PCB 333A structural accelerometers (sensitivity 100 mV/g) in combination with three PCB 433A structural signal conditioners. The structure is excited using an instrumented impact hammer of type PCB 086C03 (mass 0.136 kg). Acceleration signals were recorded with a sampling frequency f_s = 1651.6 Hz. Additional measurement specifications are presented in Marchelli et al. [12]. For each setup in Table 4, the structure is excited with the hammer at the top floor along the x- and y-direction, in correspondence with the points indicated in Figure 3(a). The test structure was hit at some distance from the symmetry axes to enable the identification of the torsional modes. The arrangement of the accelerometers is displayed in Figure 3(b) and 3(c). The vertical acceleration is recorded at the base floor; the sensors were placed at the positions at which the springs are connected. For the other floors, two sensors were applied in x-direction and one sensor in y-direction. The applied sensor setup allows for the identification of the bending mode-shapes in both directions, as well as the torsional mode shapes.

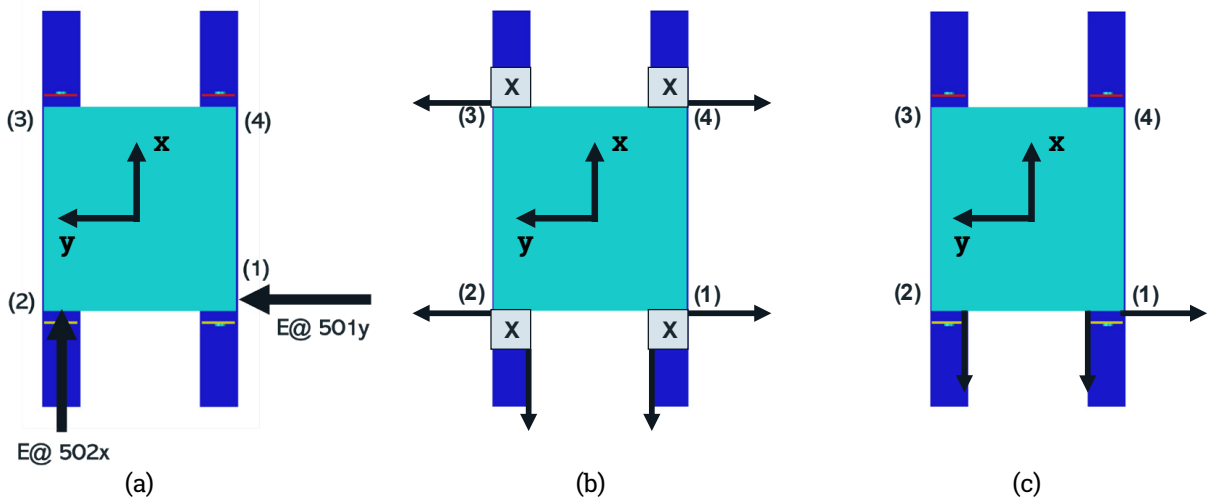

Figure 3: Schematic drawing showing (a) the directions of excitation, (b) the accelerometer arrangement at the base floor, and (c) the accelerometer arrangement at floors 1-5.

The MACEC 3.4 [13] MATLAB toolbox was utilised for data processing. Natural frequencies and mode shapes were identified through the Combined Subspace Identification, an OMAX technique. The resulting accelerations and force signals are processed using the reference-based data-driven combined deterministic-stochastic subspace identification (CSI data/ref) algorithm. Half the number of block rows in the Hankel matrices is taken as $i = 200$ [14]. The post-processing phase consisted of a comparison of the modal properties identified among the setups. This is useful to assess the reliability of the measurements and to obtain some understanding on how the base boundary conditions and the cross-sections of the strips affect the modal characteristics. Setup 01 with the fixed base conditions is the reference for the comparison. The complete description of data processing is provided in Marchelli et al. [12].

3.3 Finite element model

A Finite Element (FE) model of the test structure was constructed using Stabil 3.1 [15], a MATLAB Finite Element toolbox. The FE models are illustrated in Figure 4. The FE types employed for the discretization are the Euler-Bernoulli $beam$ and the $shell4$, a bi-linear membrane element obtained through four overlaid Discrete Kirchhoff Triangle (DKT) elements for the bending stiffness. The columns are modelled with $beam$ elements and the plates with $shell4$ elements. The mechanical properties of the columns and plates are: Young's modulus E = 210000 N/mm^2, Poisson coefficient ν = 0.3, and density ρ = 7850 kg/m^3. The masses of bolts, nodes, rings, amplifiers and sensors are included. More information about the setup of the FE models is provided by Marchelli et al. [12].

In the initial stage, simplified models were built to verify the agreement and evolution of the modal characteristics while increasing the level of detail. Firstly, a lumped-parameter shear building model was developed and then compared with a 2D and 3D FE model, all illustrated in Figure 4. Results of these models are provided and discussed in Marchelli et al. [12]. The results of the 3D FE model are discussed in this paper. An important modelling aspect consisted of including the influence of the corner connectors, which increase the local stiffness of the structure. The local thickness of the corner element was added to the thickness of the columns and plates in the contact area.

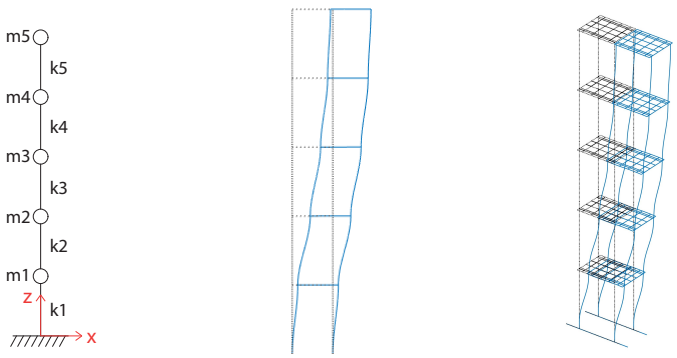

Figure 4: Schematic drawings of the models: (a) lumped-parameter shear building model, (b) 2D FE shear model, and (c) 3D FE model of the test structure.

3.4 Model updating

The parameters that were studied with model updating were:

- the Young's modulus E of the corner connectors between the plates and the columns, and
- the axial and shear stiffness of the bobbin springs at the base.

The first five modal characteristics were employed. This allows for a cross-validation with the higher modes, in order to verify that the model updating results in a better agreement for these modes. The model updating is formulated as a nonlinear least squares problem, considering the mismatch between the predicted and measured natural frequencies and mode shapes. The optimisation problem is solved using the MATLAB solver $lsqnonlin$, minimising the cost function formulated as follows:

$$F(\boldsymbol{\theta}) = \frac{1}{2}||\boldsymbol{\eta}(\boldsymbol{\theta})||_2^2 \tag{1}$$

where the residual vector $\boldsymbol{\eta}$ includes discrepancies computed both for eigenvalues and eigenvectors and can be partitioned respectively as $\boldsymbol{\eta} = \{\boldsymbol{\eta}_\omega; \boldsymbol{\eta}_\phi\}$. Mode matching is necessary for the pairing of predicted and experimental modal characteristics during the updating process and was done with:

$$a\left|1 - \frac{\omega_i(\boldsymbol{\theta})}{\overline{\omega}_j}\right| + b(1 - MAC(\boldsymbol{\phi}_i(\boldsymbol{\theta}), \overline{\boldsymbol{\phi}}_j) \tag{2}$$

where $\overline{\omega}$ and $\overline{\boldsymbol{\phi}}$ are the angular natural frequencies and mode shapes measured in the experiments, $\omega_i(\boldsymbol{\theta})$ and $\boldsymbol{\phi}_i(\boldsymbol{\theta})$ are those of the model that depend on the set of parameters $\boldsymbol{\theta}$ of the model, α and β are weighting factors for the contributions of frequencies and mode shapes.

The optimisation problem is formulated in terms of dimensionless correction factors on the physical variables, rather than the variables themselves, for a better conditioning of the optimisation problem. The scaling to dimensionless parameters removes any effect of different orders of magnitude of the updating variables. For example, a correction factor θ_k of the Young's modulus at the kth iteration is defined as:

$$E_k = \theta_k E_0 \tag{3}$$

where E_0 is the initial guess value for the Young's modulus in the FE model and E_k is Young's modulus of the FE system at the kth iteration. Before each update, a sensitivity analysis was carried out, to verify to what extent the selected parameters affected the modal characteristics. The results of the sensitivity analyses are reported in Marchelli et al. [12]. The model updating was first conducted for fixed base conditions, to remove the uncertainties of the base and to focus on the corner connections between the elements. For the updating of the corner connectors, a distinction was made between the Young's modulus E of the part of the corner connectors in contact with the columns and the part in contact with the plates. This procedure aims to detect where the impact of the corner connectors is more significant on the stiffness of the structure. Figure 5 illustrates this concept.

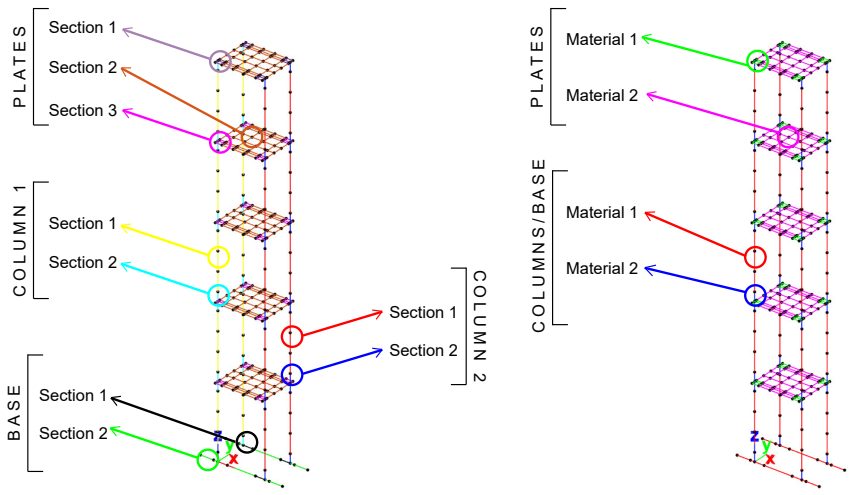

Figure 5: Schematic drawings of the applied sections in the model (left) and the materials employed for columns, plates and at the base (right).

On the left side, all the employed sections of the FE model are visible, whereas, on the opposite side, two distinct materials in terms of Young's modulus are used per strip and column. This allows updating separately the coefficient θ_c that multiplies the modulus of the column part in contact with the corner connector, and θ_p that multiplies the modulus of the part of the plates in contact with the corner connectors, without modifying the modulus of the other elements. The initial E-moduli are set to 210000 N/mm^2, as in the rest of the test structure.

After the updating for the fixed base conditions, studies were performed for the stiff base conditions and the soft base conditions. In these studies, the axial and shear stiffness of the bobbin springs were updated using the coefficients θ_1 (shear) and θ_2 (axial), while the other parameters of the model were kept at the same values as for the fixed base configuration.

4 Results and discussion

4.1 Modal properties test structure

Table 5 specifies the measured mode shapes and the corresponding natural frequencies $\overline{f}$ and modal damping ratios $\overline{\xi}$ for setup 01. The natural frequencies f computed with the FE model are provided as well. The order of the modal characteristics reflects the asymmetrical stiffness of the structure in x- and y-direction, which is due to the orientation of the column cross-sections. The mode shapes of the fundamental bending modes in x- and y-direction and in torsion are shown in Figure 6 for the test structure and in Figure 7 for the FE model. The modes of different configurations were matched based on the MAC values, using a threshold of 0.6 for mode matching. Table 6 gives the modal damping ratios for three different model setups, all having the same column arrangement but with different base boundary conditions (fixed, stiff and soft). For setup 05, with fixed base conditions, the damping values range between 0.165-0.263%. Setup 05 exhibits higher values of modal damping compared to setup 01, except for the damping determined for mode shapes by1 and by2, which remain unchanged. Torsional modes t1 and t2 also show a smaller increase compared to the bending along the x-axis mode-shapes. This change is due to the column configuration in setup 01, where the structure is less stiff due to the higher proportion of 1.5 mm thick columns. The comparison of modal damping ratios obtained for setup 01 and 05 indicates that a higher stiffness in the test structure corresponds to a higher modal damping ratio. Base boundary conditions also affect the modal damping. With stiff springs (setup 14), modal damping values vary between 0.187-1.563 %, while with soft springs (setup 10) the damping values range between 0.262-2.450 %. The larger flexibility at the base results in a higher modal damping, especially for the first three modes bx1, by1 and t1.

Table 5: Modal characteristics of the test structure and the FE model for setup 01.

Mode-shape	Label	Mode type	$\overline{f}$ [Hz]	$\overline{\xi}$ [%]	f [Hz]	$\frac{\overline{f}-f}{\overline{f}}$ [%]
01	bx1	Bending along x	3.92	0.136	3.90	+0.51
02	by1	Bending along y	6.83	0.244	6.50	+4.69
03	t1	Torsional	9.07	0.156	9.21	-1.54
04	bx2	Bending along x	11.78	0.188	11.63	+1.27
05	bx3	Bending along x	19.36	0.160	19.04	+0.00
06	bx4	Bending along x	25.66	0.177	25.44	+0.86
07	by2	Bending along y	27.55	0.263	33.32	-20.94
08	bx5	Bending along x	29.90	0.169	29.88	+0.07
09	t2	Torsional	32.02	0.160	37.89	-18.33

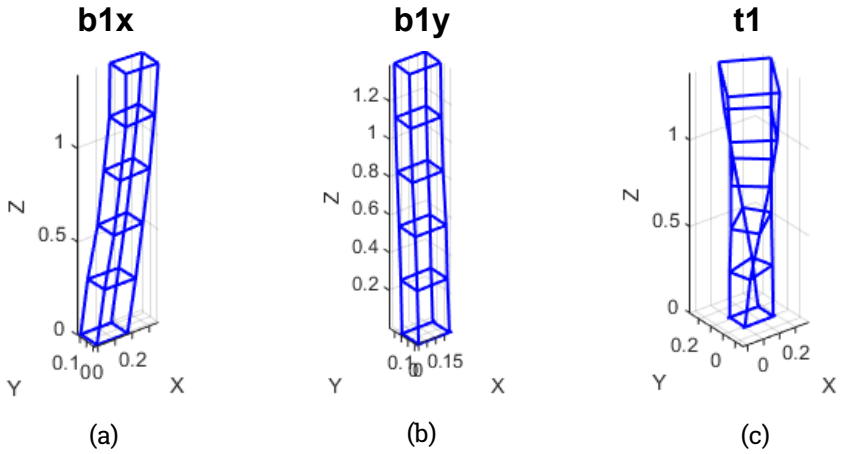

Figure 6: Three of the measured mode-shapes: (a) bending mode along x-axis (3.92 Hz), (b) bending mode along y-axis (6.83 Hz) and (c) torsional mode (9.07 Hz).

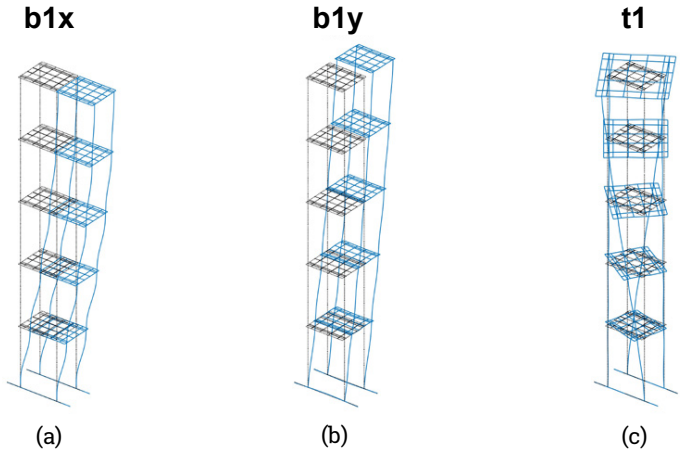

Figure 7: Three of the FE model mode shapes: (a) bending mode along x-axis (3.90 Hz), (b) bending mode along y-axis (6.50 Hz) and (c) torsional mode (9.21 Hz).

Table 6: Modal damping ratios for the test structure with the fixed base (setup 05), with stiff springs (setup 14), and with soft springs (setup 10).

Mode	Label	Setup 05 (fixed)	Setup 14 (stiff)	Setup 10 (soft)
01	bx1	0.197	0.329	1.229
02	by1	0.244	1.563	2.450
03	t1	0.165	0.258	0.440
04	bx2	0.209	0.228	0.368
05	bx3	0.185	0.200	0.340
06	bx4	0.203	0.187	0.344
07	by2	0.263	0.750	0.900
08	bx5	0.165	0.193	0.262
09	t2	0.168	0.265	-

4.2 Fixed base results

Figure 8(a) compares the natural frequencies obtained from the measurements on the test structure (setup 01) with those estimated with the FE model. Figure 8(b) compares measured and modelled mode shapes using the MAC value. The natural frequencies and mode shapes obtained in the measurements generally compare well with those estimated with the 3D FE model. Lower MAC values are observed for modes by1, by2, and t2, which also show the largest discrepancies in natural frequencies. For modes by2 and t2, the natural frequencies determined with the FE model are more than 15 % larger than those measured on the test structure. For these modes, the test structure has a higher stiffness than the FE model. Model updating was carried out, but did not result in a more optimal solution for the FE model, as the first 5 modes used in the model updating already agreed well. Marchelli et al. [12] provides more information about the performed model updating on the fixed base test structure.

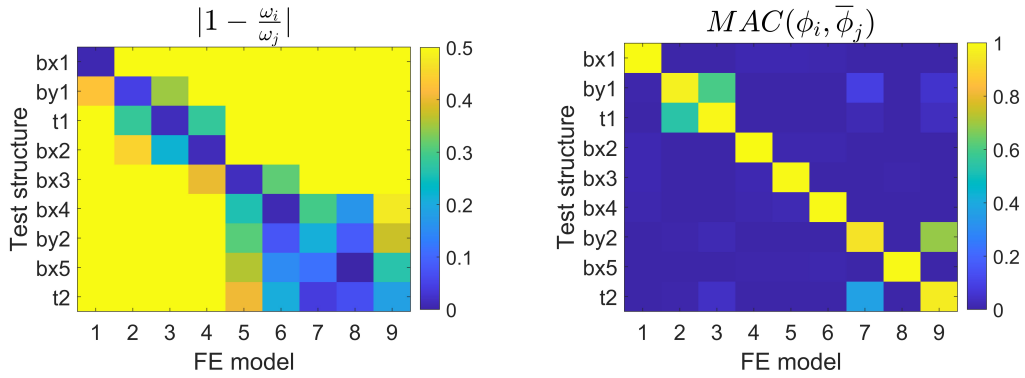

Figure 8: Comparison of the modal characteristics of the test structure and FE model: (a) natural frequencies and (b) mode shapes.

4.3 Stiff spring base results

Figure 9(a) and (b) show the comparison between the FE model and the test structure for setup 12 before model updating. The differences in natural frequencies are provided in Table 7. The largest differences are observed for modes bx1 and by1, with the FE model giving lower natural frequencies than the measured values. For modes by2 and t2 the FE model estimated larger natural frequencies than those measured. The model updating for the stiff spring configuration (setup 12) resulted in a converged solution with $\theta_1 = 0.6754$ and $\theta_2 = 1.5938$. This indicates that the initial shear stiffness (θ_1) of the springs was larger than the updated value, while the initial axial stiffness (θ_2) was smaller. The first 5 modes were used in the model updating, which explains the relatively small errors observed for these modes in Table 7. The differences observed for the last 5 modes after model updating are about the same as before the model updating. This shows a lack of cross-validation and indicates there are still some modelling inaccuracies in the 3D FE model. The differences observed for modes by2 and t2 are particularly large. These are the same modes that were found to show large deviations for the fixed base configuration, which suggests that the modelling inaccuracies are not related to the base conditions, but to the upper steel part of the test structure. Table 8 presents the residuals of the first 5 modes for natural frequencies and mode shapes. For setups 13, 14, and 15, the values were computed with the values of the parameters θ_1 and θ_2 that were obtained with the model updating performed for setup 12. The final column on the right side of Table 8 displays the values of the objective function. A comparison of the objective function values before and after updating shows that these have reduced. This reduction is mainly due to the reduction of the residuals in terms of natural frequencies (see Table 8); the relative residual reduction of the mode shapes is negligible in comparison. This suggests that for the stiff spring base, the influence of the mode shapes on the model updating is limited, and that the updating process for this base configuration appears mainly determined by the natural frequencies.

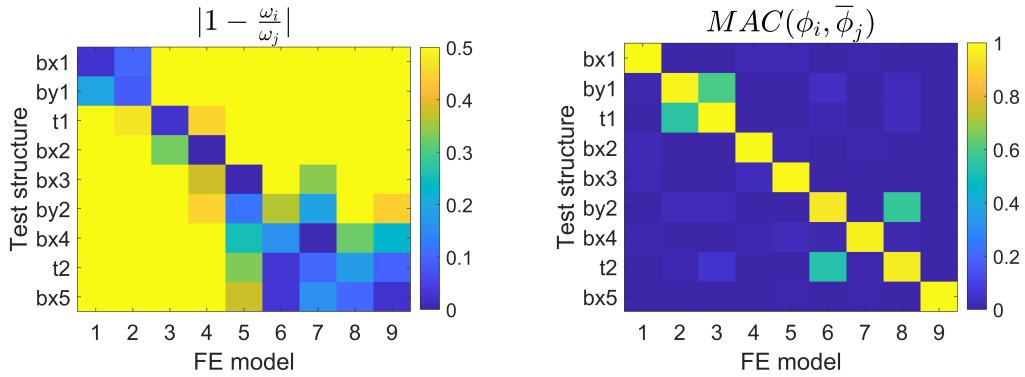

Figure 9: Comparison of the modal characteristics of the test structure and FE model before model updating: (a) natural frequencies and (b) mode shapes.

Table 7: Natural frequencies measured for the test structure $\overline{f}$ and estimated with the FE model f, and the relative difference before and after model updating.

Mode-shape	$\overline{f}$ [Hz]	f [Hz] Before	f [Hz] After	$\frac{\overline{f}-f}{\overline{f}}$ [%] Before	$\frac{\overline{f}-f}{\overline{f}}$ [%] After
bx1	4.28	2.82	4.25	+34.11	+0.70
by1	5.16	2.05	5.18	+60.27	-0.00
t1	8.93	8.32	8.75	+6.83	+2.02
bx2	12.90	12.74	12.95	+1.24	-0.39
bx3	20.83	20.53	20.66	+1.44	+0.82
by2	23.49	31.00	31.69	-31.97	-34.91
bx4	27.66	27.92	27.87	-0.94	-0.76
t2	31.01	36.13	35.82	-16.51	-15.51
bx5	33.10	33.94	33.92	-2.54	-2.48

Table 8: Squared residuals computed for natural frequencies and mode-shapes before and after the updating for setups with stiff springs at the base setting $a = 1$ and $b = 1$ with $\theta_1 = 0.6765$ and $\theta_2 = 1.5938$.
*The residuals for setup 13, 14 and 15 after updating were determined with θ_1 and θ_2 of setup 12.

	$a\sum_{i=1}^{5}(1-\omega_i/\overline{\omega_i})^2$		$b\sum_{i=1}^{5}(\overline{\phi_i}-\phi_i)^2$		Obj.func.	
Setup	Before	After	Before	After	Before	After
12	0.0091	0.0005	0.0548	0.0533	0.0639	0.0538
13*	0.0084	0.0004	0.0496	0.0495	0.0580	0.0499
14*	0.0085	0.0004	0.0504	0.0491	0.0589	0.0494
15*	0.0088	0.0005	0.0530	0.0520	0.0618	0.0525

4.4 Soft spring base results

The model updating with soft springs at the base was performed for setup 10. Figure 10 and Table 9 compare the natural frequencies and mode shapes of the FE model and the test structure before model updating, after model updating with a = b = 1, and after model updating with a = 1 and b = 0.1. The natural frequencies and mode shapes determined with the FE model before the model updating compare well with those from

the measurements. Only mode by1 and by2 show significant differences. Figure 10(b) and (e) show that the model updating performed with a = b = 1 results in a better prediction of the by1 natural frequency and of the MAC value for the by2 mode. However, the natural frequency error for mode by2 almost doubles. An additional model updating was performed with a = 1 and b = 0.1. Figure 10 (c) and (f) present the results for the natural frequencies and mode shapes. Now the opposite is observed, with a better estimation of the by2 natural frequency, but a worse prediction of the mode shape.

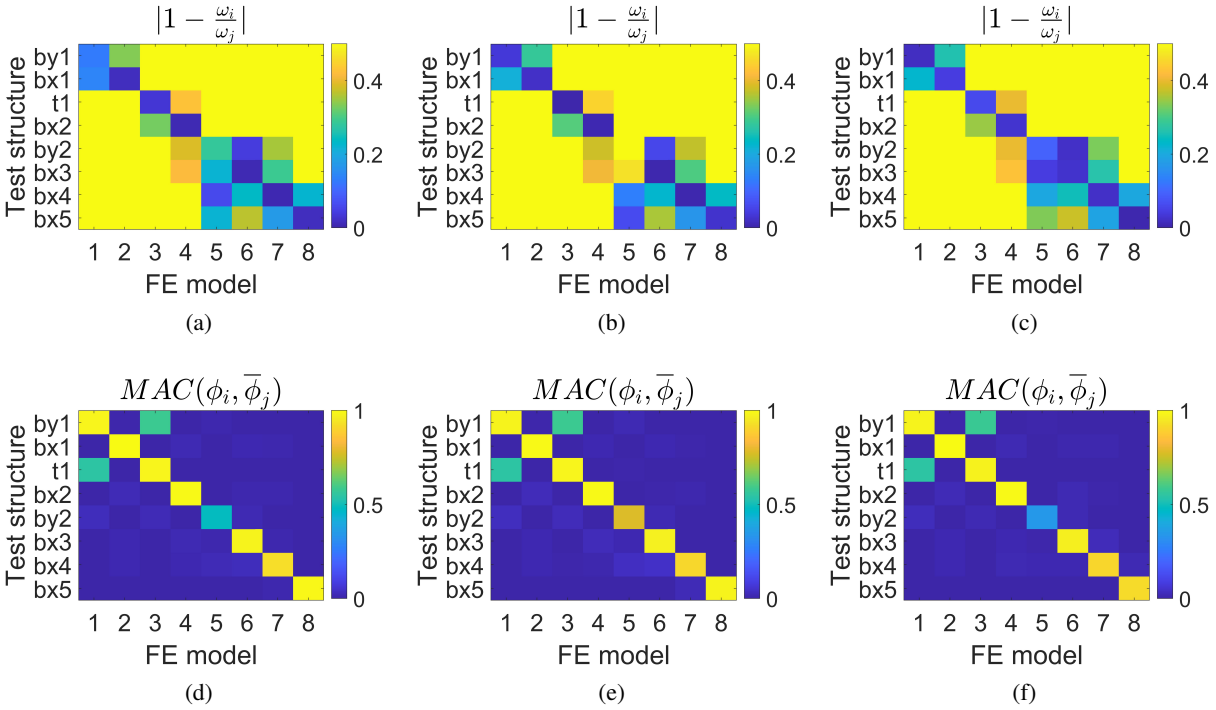

Figure 10: Comparison of natural frequencies and MAC values for the soft spring base (setup 10): (a, d) before model updating, (b, e) after model updating (a = b = 1), (c, f) after model updating (a = 1 and b = 0.1).

Table 9: Natural frequencies of the test structure $\overline{f}$ and the FE model f before and after model updating.

Mode	$\overline{f}$ [Hz]	f [Hz] Before	f [Hz] After a = 1 b = 1	f [Hz] After a = 1 b = 0.1	$\frac{\overline{f}-f}{\overline{f}}$ [%] Before	$\frac{\overline{f}-f}{\overline{f}}$ [%] After. a = 1 b = 1	$\frac{\overline{f}-f}{\overline{f}}$ [%] After a = 1 b = 0.1
by1	2.53	2.86	2.62	2.58	-13.04	-3.56	-1.98
bx1	3.33	3.38	3.26	3.19	-1.50	+2.10	+4.20
t1	8.37	8.11	8.33	7.86	+3.12	+0.48	+6.09
bx2	12.05	11.94	12.13	11.71	+0.91	-0.66	+2.82
by2	19.47	24.97	30.01	21.32	-28.25	-54.13	-9.50
bx3	20.45	20.27	20.56	19.93	+0.88	-0.54	+2.54
bx4	26.54	26.38	26.69	25.93	+0.60	-0.57	+2.30
bx5	31.97	32.48	32.82	31.82	-1.60	-2.66	+0.47

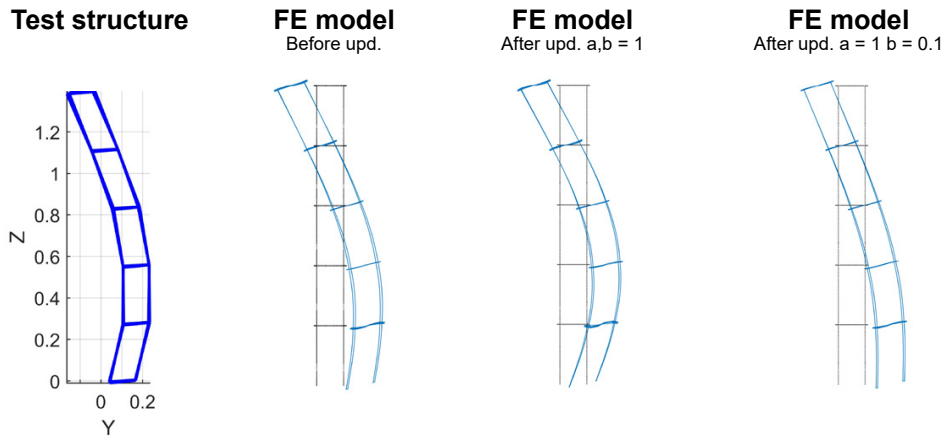

Figure 11: The by2 mode-shape for setup 10 (soft) determined for the test structure and for the FE model.

The same by2 mode showed large deviations for the fixed and stiff spring base configuration. Figure 11 shows the by2 mode shapes determined from the measurements on the test structure, as well as those obtained with the FE model before and after model updating. Three notable differences are observed:

- The floors in the measured mode shape are less inclined than those in the modelled mode shapes,
- the corners in the measured mode shape appear less stiff than in the modelled mode shapes, and
- the displacement at the base differs significantly for the measured and modelled mode shapes.

The first two differences might indicate that the applied stiffness of the corner connectors is too high. However, the measured mode shape in Figure 11 does not contain information on the vertical modal displacements, except for the base. The modelled mode shapes indicate significant vertical modal displacements, also at the higher floor levels, which are not considered in the model updating. This information is required to allow for a better consideration of the mode shapes in the model updating, and could help determine why the higher modes (particularly mode by2 and t2) obtained with the FE model for the fixed base and stiff spring base do not match well with the measured modes. The differences in base displacement are mainly related to the shear stiffness of the springs. Depending on the settings, the results vary between $\theta_1 = 3.2$, for a = b = 1, and $\theta_1 = 0.7$, for a = 1 and b = 0.1. The results for θ_2 are very similar, with $\theta_2 = 0.8$ for a = b = 1, and $\theta_2 = 0.79$ for a = 1 and b = 0.1. These results suggest that the model updating provides a reliable estimate for the axial spring stiffness, but that the estimate for the shear spring stiffness is not reliable. More modal information appears needed to make a reliable estimate of the shear stiffness using model updating.

5 Conclusion

An accurate estimation of the stiffness of both the superstructure and the foundation of a high-rise building is crucial for predicting its fundamental natural frequency. Through model updating, we aimed to estimate these global structural parameters. However, determining the reliability of the updated building and foundation stiffness estimates proved challenging. To better understand the effective application of model updating on such structures, a laboratory experiment was conducted using a scale model of a high-rise building. A dataset of modal properties for various configurations of this test structure was generated, enabling a sensitivity analysis of different structural parameters. Model updating was applied to three test configurations: a fixed base, a stiff spring base, and a soft spring base. Results indicated that increasing the base flexibility makes the identified shear spring stiffness highly sensitive to model updating settings, while the axial spring stiffness remains stable. This suggests model updating can effectively estimate the in-situ rotational foundation stiffness of high-rise buildings, but is less suitable for the horizontal foundation stiffness. Future research will study in mode detail the application of model updating to both the test structure dataset and in-situ structures, for example looking into optimal measurement setups and necessary modelling details.

Readers interested in using the test structure dataset are encouraged to contact the authors by email. The dataset and technical specifications of the test structure will be provided upon request to support further research in vibration-based structural identification techniques.

References

[1] A. Jeary, *The dynamic behaviour of the Arts Tower, University of Sheffield, and its implications to wind loading and occupant reaction*. Building Research Establishment, 1978.

[2] B. Ellis and J. Littler, "Lessons from dynamic testing of buildings," *Proceedings of Structural Assessment based on full and large-scale testing*, 1987.

[3] J. Y. Kim, E. Yu, D. Y. Kim, and S.-D. Kim, "Calibration of analytical models to assess wind-induced acceleration responses of tall buildings in serviceability level," *Eng. Struct.*, vol. 31, no. 9, pp. 2086–2096, 2009.

[4] M. Friswell and J. Mottershead, "Finite element model updating in structural dynamics, kluwer academic publishers," 1995.

[5] B. Ellis, "An assessment of the accuracy of predicting the fundamental natural frequencies of buildings and the implications concerning the dynamic analysis of structures," *Proceedings of the Institution of Civil Engineers*, vol. 69, no. 3, pp. 763–776, 1980.

[6] T. Kijewski-Correa, J. Kilpatrick, A. Kareem, D.-K. Kwon, R. Bashor, M. Kochly, B. S. Young, A. Abdelrazaq, J. Galsworthy, N. Isyumov *et al.*, "Validating wind-induced response of tall buildings: Synopsis of the chicago full-scale monitoring program," *Journal of Structural Engineering*, vol. 132, no. 10, pp. 1509–1523, 2006.

[7] Y. Zhou, Y. Zhou, W. Yi, T. Chen, D. Tan, and S. Mi, "Operational modal analysis and rational finite-element model selection for ten high-rise buildings based on on-site ambient vibration measurements," *Journal of Performance of Constructed Facilities*, vol. 31, no. 5, p. 04017043, 2017.

[8] J. Wu and Q. Li, "Finite element model updating for a high-rise structure based on ambient vibration measurements," *Engineering Structures*, vol. 26, no. 7, pp. 979–990, 2004.

[9] C. E. Ventura, R. Brincker, E. Dascotte, and P. Andersen, "Fem updating of the heritage court building structure," in *Proceedings of IMAC 19: A Conference on Structural Dynamics: february 5-8, 2001, Hyatt Orlando, Kissimmee, Florida, 2001*. Society for Experimental Mechanics, 2001, pp. 324–330.

[10] K. Kaynardağ and S. Soyöz, "'structural health monitoring of a tall building," in *Second European Conference On Earthquake Engineering And Seismology*, 2014, pp. 25–29.

[11] D. Moretti, A. Bronkhorst, and C. Geurts, "Identification of the structural properties of a high-rise building," in *Proceedings ISMA2022, Leuven, Belgium*, 2022.

[12] E. Marchelli, K. Maes, F. Tubino, G. Piccardo, O. Bronkhorst, D. Moretti, and G. Lombaert, "Reducing the uncertainty in dynamic models of high-rise buildings by means of parameter identification," Master's thesis, Università degli Studi di Genova, Genova, GE, 2023.

[13] B. Peeters, B. Van den Branden, and G. De Roeck, "Output-only modal analysis: a gui for matlab," in *2nd Benelux Matlab Users Conference, Brussels, Belgium*, 1999.

[14] E. Reynders and G. D. Roeck, "Reference-based combined deterministic–stochastic subspace identification for experimental and operational modal analysis," *Mechanical Systems and Signal Processing*, vol. 22, no. 3, pp. 617–637, 2008.

[15] S. François, M. Schevenels, D. Dooms, M. Jansen, J. Wambacq, G. Lombaert, G. Degrande, and G. De Roeck, "Stabil: An educational matlab toolbox for static and dynamic structural analysis," *Computer Applications in Engineering Education*, vol. 29, no. 5, pp. 1372–1389, 2021.